Social network architecture and the tempo of cumulative cultural evolution

Mauricio Cantor[1,2,†,*], Michael C. Chimento[3,†], Simeon Q. Smeele[3,4,†], Peng He[5,6,7], Danai Papageorgiou[5,6,7], Lucy M. Aplin[3,6,^,*], Damien R. Farine[5,6,7,^]

[1] Department for the Ecology of Animal Societies, Max Planck Institute of Animal Behavior, Konstanz, Germany

[2] Departamento de Ecologia e Zoologia, Universidade Federal de Santa Catarina, Florianópolis, Brazil

[3] Cognitive & Cultural Ecology Research Group, Max Planck Institute of Animal Behavior, Radolfzell, Germany

[4] Department of Human Behavior, Ecology and Culture, Max Planck Institute for Evolutionary Anthropology, Leipzig, Germany

[5] Department of Collective Behaviour, Max Planck Institute of Animal Behavior, Konstanz, Germany

[6] Department of Biology, University of Konstanz, Konstanz, Germany

[7] Centre for the Advanced Study of Collective Behaviour, University of Konstanz, Konstanz, Germany

^Joint senior authors; †Joint first authors, arranged alphabetically

* Corresponding Authors: Mauricio Cantor. Department for the Ecology of Animal Societies, Max Planck Institute of Animal Behavior, Am Obstberg 1, Radolfzell 78315, Germany; Lucy M. Aplin. Cognitive & Cultural Ecology Research Group, Max Planck Institute of Animal Behavior, Am Obstberg 1, Radolfzell 78315, Germany, Phone: +49 7732 1501-13. Email: mcantor@ab.mpg.de, laplin@ab.mpg.de

Abstract

The ability to build upon previous knowledge—cumulative cultural evolution (CCE)—is a hallmark of human societies. While CCE depends on the interaction between social systems, cognition and the environment, there is increasing evidence that CCE is facilitated by larger and more structured societies. However, the relative importance of social network architecture as an additional factor shaping CCE remains unclear. By simulating innovation and diffusion of cultural traits in populations with stereotyped social structures, we disentangle the relative contributions of network architecture from those of population size and connectivity. We demonstrate that while multilevel societies can promote the recombination of cultural traits into high-value products, they also hinder spread and make products more likely to go extinct. We find that transmission mechanisms are therefore critical in determining the outcomes of CCE. Our results highlight the complex interaction between population size, structure and transmission mechanisms, with important implications for future research.

Keywords

Cultural evolution | Cultural complexity | Multilevel societies | Small-world networks | Social structure

Introduction

Cumulative cultural evolution—where iterative innovations and social transmission generate cultural accumulation over time [1-3]—is key to the human's ecological success and worldwide distribution [4,5]. While CCE fundamentally depends on the interplay between cognition and social learning mechanisms [1], it is increasingly clear that demography can modulate the rate of cultural evolution [6-9]. Large population sizes [10,11], greater population turnover, and more densely connected societies [3,12] can all provide greater innovative potential, more learning models, faster diffusion, and reduced extinction risk of useful innovations [7,13-15]. For example, increasing population density as well as migration of hunter-gatherers during the upper Paleolithic transition led to the explosion of culture that forms the basis of modern human

55 societies [8,15]. Yet, it remains unclear how variation in the wiring of these social connections
56 shape the tempo of cumulative cultural evolution.
57
58 Network architecture—here defined as a social structure with a characteristic set of properties—
59 can shape transmission of behaviours, thus setting the tempo of CCE—here defined as the rate of
60 cultural recombination events. For example, architectures with low network connectivity (i.e.
61 density; proportion of realised connections), high clustering (tendency of connected individuals to
62 share the same social neighbours) and high modularity (tendency of the network to contain sets of
63 individuals more connected to each other than with others) slow down the spread of information
64 across populations [16-18]. Slower spread can then potentially favour greater cultural diversity by
65 allowing multiple cultural lineages to arise in populations before any one lineage dominates
66 [19,20]. While previous work has largely focused on how new behaviours spread through a social
67 network [16,17] to establish cultures [20,21] and how cultural traits can generate a feedback
68 shaping network structure [18,22], more recently it has been argued that emergent network
69 properties could affect CCE [12,14,19] by shaping how new traits are produced, recombined, and
70 maintained [14]. For example, partial connectivity facilitates the emergence of multiple cultural
71 lineages in parallel [20], which is required for achieving cultural accumulation, but partially-
72 connected networks suffer from cultural loss if connectivity is too low for new innovations to
73 spread [14]. By contrast, full connectivity facilitates rapid spread of new innovations, but can
74 prevent the accumulation of alternative cultural traits [12,14]. However, within a given level of
75 connectivity, how connections are structured—the social network architecture—could also impact
76 CCE by influencing how fast and widely information can spread.
77
78 Because network architecture can shape the effect of connectivity on diffusion dynamics [23], those
79 architectures that balance the ability for cultural accumulation together with the recombination of
80 different cultural traits should have a selective advantage in facilitating CCE [19]. Multilevel
81 societies, such as those in modern hunter-gatherers, feature high clustering and nested modularity.
82 These network properties are expected to favour CCE by allowing coexistence of multiple cultural
83 traits in different parts of the network, and for different cultural lineages to come into contact to
84 allow combinations from lineages to produce new traits [19]. Multilevel societies have been

demonstrated to accelerate CCE when compared to fully connected networks [19]. However, when considering their potential for facilitating CCE, multilevel and fully-connected networks represent possible endpoints along a continuum of possible architectures. Here, we ask how a range of social network architectures can affect the tempo of CCE within a given population size and number, or density, of social connections within that population. Our approach allows us to explicitly disentangle the relative contribution of network architecture from those of connectivity and population size.

Results

We generated networks with six different architectures—random, small-world, lattice, modular, modular lattice, and multilevel—capturing different levels and combinations of clustering and modularity (**Fig. 1A**). We expressed these network architectures in populations with different sizes and densities of connections (average degree), where all individuals in the network had the same degree. We then used the agent-based model implemented by Migliano et al. [19] (hereafter model 1), inspired by the experiment of Derex & Boyd [12], to explore how network architecture affects time to cultural recombination (i.e. tempo) and the diversity of cultural traits. Briefly, this model allows innovations of cultural products to take place along two cultural lineages, with the knowledge of new products being spread to all social connections (one-to-many diffusion). Once a

high level of product diversity has been reached in both lineages, agents can recombine each lineage's products into one with a final higher payoff product (hereafter 'recombination').

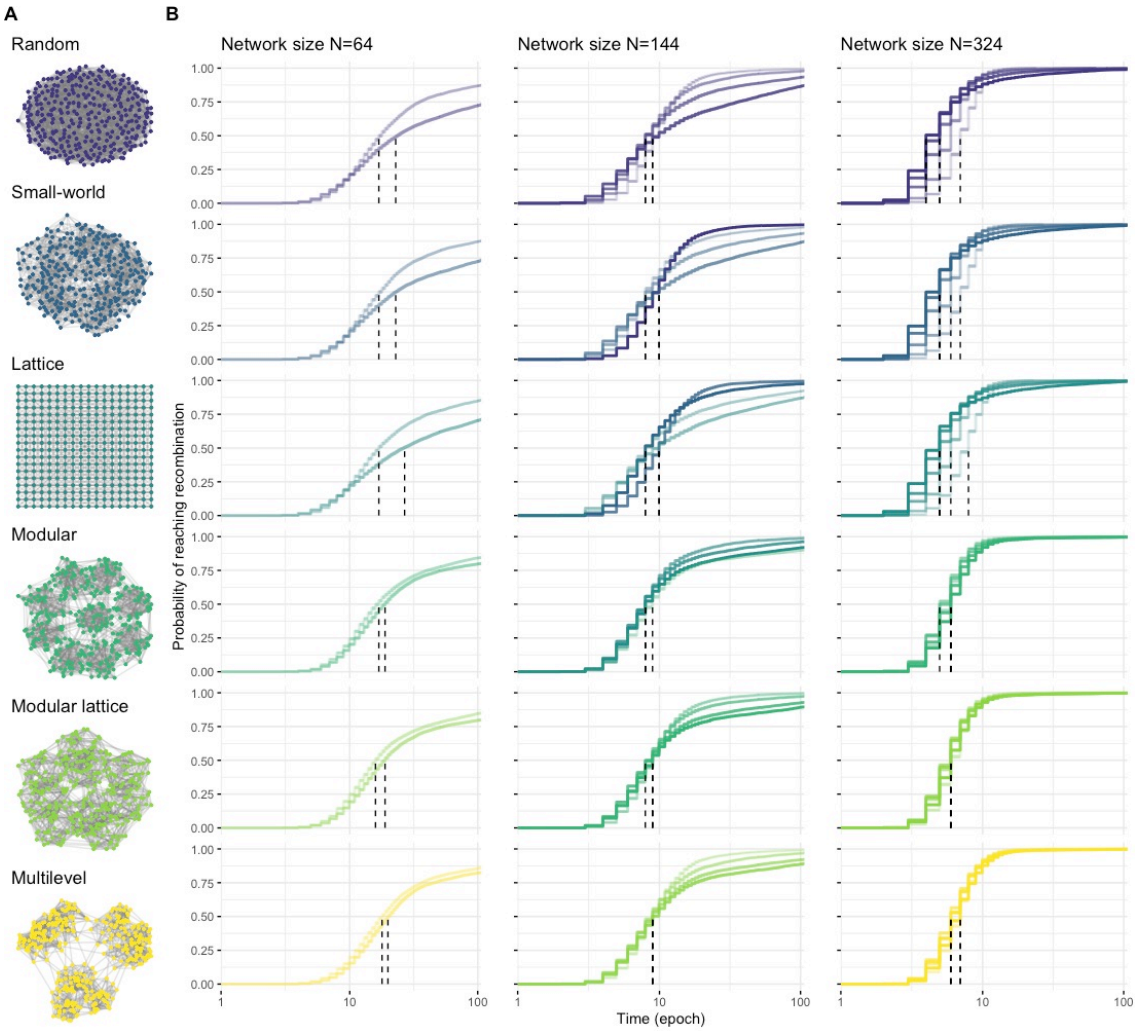

Figure 1. Social network architectures, and the time to recombination for each architecture across population sizes and levels of connectivity using model 1. (A) Network architectures vary in clustering and modularity: Random (unclustered C=0.03, non-modular Q=0.24), small-world (clustered C=0.52, medium-modular Q=0.63), lattice (clustered C=0.45, medium-modular Q=0.54), modular (unclustered C=0.23, modular Q=0.82), modular lattices (clustered C=0.41, modular Q=0.81), multilevel (clustered C=0.42, modular Q=0.83). Each binary network depicts populations with the same number of individuals (here, N=324 nodes) that have the same number of social connections (here, degree K=12 links per node; density D=0.037) but are wired differently. **(B)** Cumulative incidence of recombination events (y-axis) as a stepwise function over time (x-axis, log epochs) for small (N=64), medium (N=144), and large population sizes (N=324). The line shading represents the amount of network connectivity (node degree K, where the lighter the shade, the smaller the degree (K$\in${8,12} for N=64; K$\in${8,12,18,24} for N=144; K$\in${8,12,18,24,30} for N=324). Vertical dashed lines indicate the median of time to

recombination (S(t)≤0.5) per network connectivity, across architectures. The time to reach recombination was truncated to 100 epochs for better visualization. Curves were calculated based on 5,000 simulations.

Confirming the effects of population size and connectivity on CCE

When comparing time to recombination, we confirm that partially connected networks outperform fully connected networks [12,14,19] **(Fig. 2A)**. A generalized linear model indicated that overall fully connected networks were, on average, 65% slower (GLM, exp(β)=1.652, t=59.208, p<.001; **Table S1**) compared to the least structured network architecture of the same size (random, N=64 taken as the intercept), with similar decreases in performance independent of size. Further, we also confirm [7] that larger populations take less time (about 40% less) to reach recombination (GLM, exp(β)=0.618, t=-68.481, p<.001) compared to networks of the same architecture and connectivity (**Figs. 1B,2, Table S2**). Larger partially-connected network architectures were less variable in their time to recombination (Quartile Coefficient of Dispersion: *QCD*=0.688 for N=64; *QCD*=0.444 for N=144; *QCD*=0.273 for N=324, **Fig. 2A**). We also found that time to recombination was optimized at intermediate densities of connections, confirming that intermediate levels of connectivity can favour CCE [14], and revealing that the optimal level of connectivity varied with population size (**Fig. 1B**). In the smallest population (N=64), sparse networks outperformed the others, but this was reversed in the largest population (N=328) (**Fig. 1B**). However, differences in time to recombination were generally small (**Fig. 1B, 2A**).

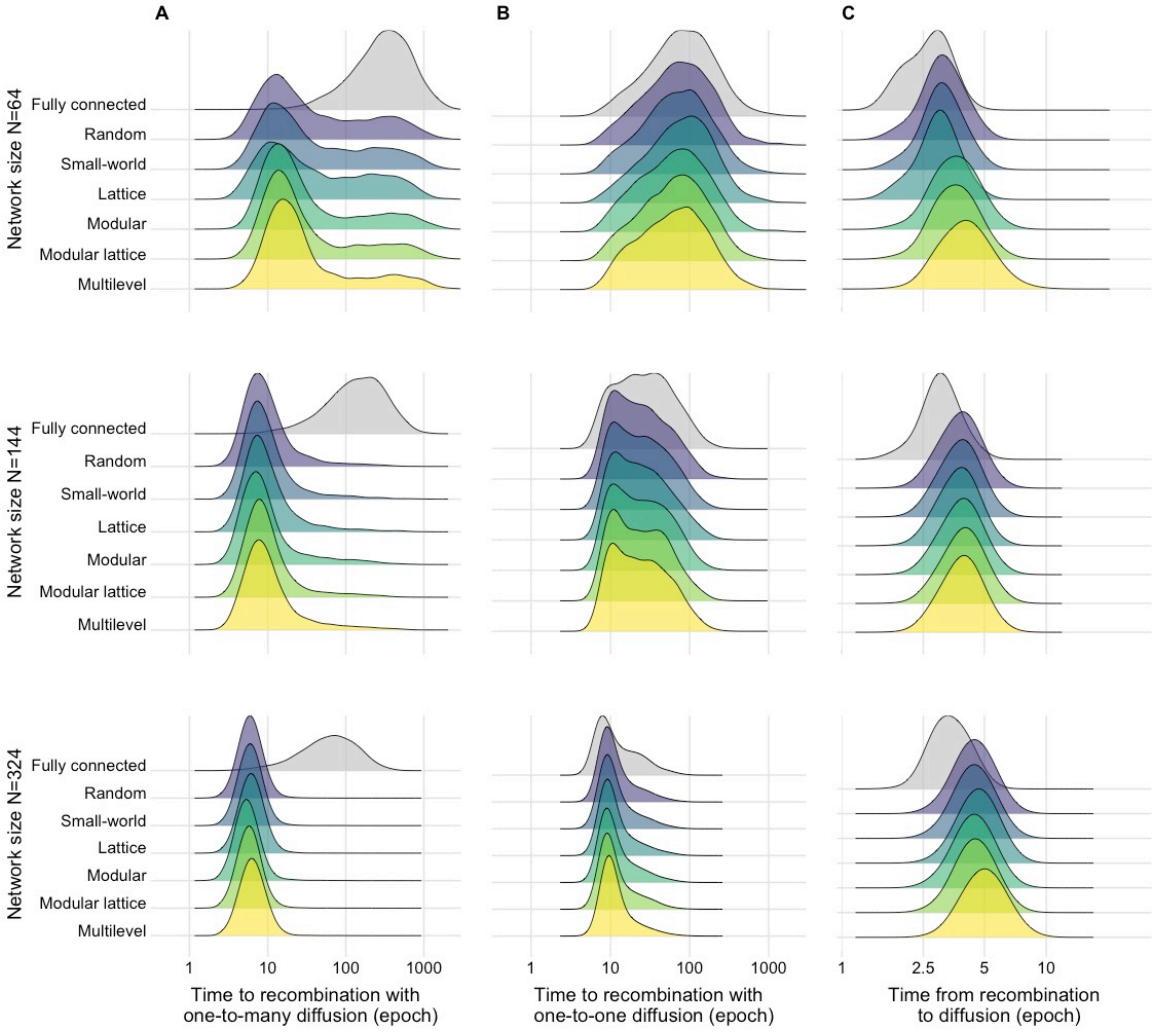

Figure 2. Time to recombination and time from recombination to diffusion across network architectures with varying sizes but a fixed degree. Comparison of the performance across the range of network architectures of the same degree (here K=12 link per node) and fully connected networks of the same size (N=64, N=144, and N=324 nodes, K=63, 143, and 323 respectively). **(A)** Time to recombination (log epochs) from 5,000 simulations with model 1 that uses a broadcast (one-to-many) diffusion dynamic. **(B)** Time to recombination (log epochs) from 5,000 simulations with model 2 that uses a dyadic (one-to-one) diffusion dynamic. **(C)** Difference between the time to recombination and the time to diffusion, where time to diffusion corresponds to the latency until the majority of the individuals in the population has information about the final higher-payoff product, from 5,000 simulations using model 2 (one-to-one diffusion). All ridges were plotted with the same bandwidth (0.18).

Architectures favouring CCE under some conditions disfavour CCE under other conditions

Under the one-to-many diffusion mechanism (model 1), multilevel, modular, and modular lattice architectures had relatively shorter times to recombination in smaller populations with greater connectivity and in larger populations with less connectivity (**Fig. 3A**). However, such network architectures performed worse than lattice, small world, and random architectures in smaller populations with less connectivity and in larger populations with greater connectivity (**Fig. 3A**). Multilevel, modular, and modular lattice architectures were optimal at lower and higher levels of connectivity in medium-sized populations (N=144, **Fig. 3A**), although connectivity generally had a lesser impact for these architectures relative to random, small-world, and lattice architectures (**Fig. 1B**). Surprisingly, multilevel performed the worst in seven out of the 11 size and connectivity combinations (**Fig. 3A**) despite having the highest clustering and modularity—properties that have been predicted to favour CCE [19]. The modular lattice architecture (which had similar modularity and clustering to multilevel architecture) performed best in the other four combinations (**Fig. 3A**). Thus, no one network architecture proved optimal, with those favoured under some conditions being disfavoured under other conditions.

The large variation in the time to recombination (**Fig. 2**) within a given combination of network architecture, population size, and density of connections suggests that the outcomes of a simulation were predominantly driven by stochastic events. The impact of such stochasticity is best revealed by the bimodal outcome for partially connected networks, which arises most often in smaller populations **(Fig. 2A)**. This bimodality occurs because there are fewer independent innovation events when there are fewer individuals, which increases the chance that cultural products all emerge from the same lineage and, therefore, that this single lineage spreads to the whole population before the other lineage is innovated. Tracking the diversity of products over time (**Figs. 4,S1**) highlights how the stochasticity in early events can affect cultural diversity, and therefore the outcomes of CCE, even within the same network architecture. Overall, measuring the tempo of CCE under one-to-many diffusion (model 1) revealed differences in the best performing architecture across population sizes and levels of connectivity (**Fig. 2A,3A**); however, these

between-architecture differences were small (range = 0.886-1.145; **Fig. 3A**), compared to the large variance in the time to recombination within architecture (**Fig. 2A**).

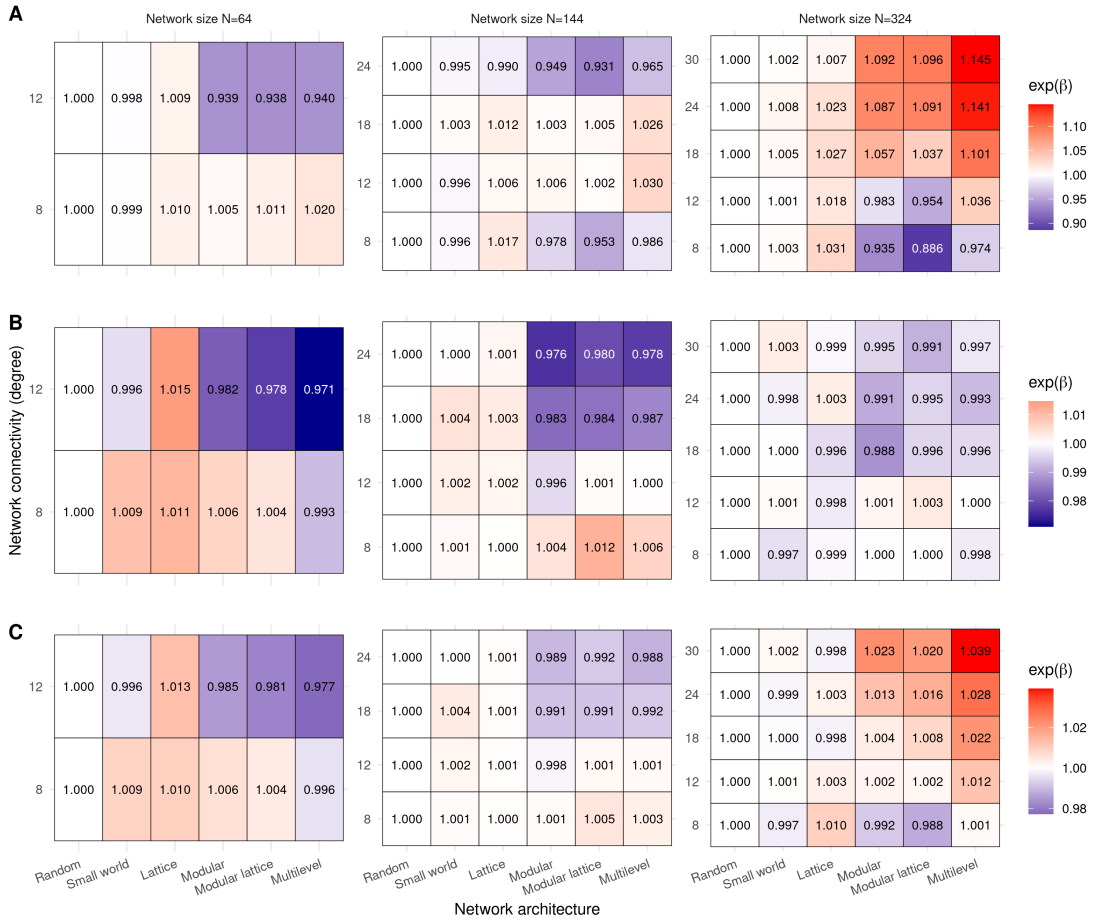

Figure 3. Relative performance of network architectures within each of the 11 combinations of population size and level of connectivity used in the simulations. Each row of each table reports the coefficient estimate of GLMs of network architecture (column) in function of the time to recombination while maintaining degree (row) and network size (box) constant. Red colours (higher coefficients) represent a poorer performance (longer latency to recombination) while blue colours represent architecture that perform better (shorter latency to recombination) for that combination of population size and level of connectivity (using random networks as the reference architecture in the GLM intercept). The relative performance of each architecture is shown for **(A)** time to recombination under a one-to-many diffusion mechanism (model 1), **(B)** time to recombination under a one-to-one diffusion mechanism (model 2), and **(C)** total time to diffusion (from simulation start until the majority of the population has information about the final higher-payoff product) under a one-to-one diffusion mechanism (model 2).

Diffusion mechanisms modify the contribution of network architecture, population size and connectivity on CCE

To identify the relative contribution of diffusion mechanisms to CCE, we extended model 1 by implementing a one-to-one diffusion mechanism (hereafter model 2). Whereas model 1 represents

an extreme scenario where information spreads instantaneously to all the contacts of a focal agent, model 2 tests another extreme in which information about discoveries spread only to a single contact at a time. Interestingly, when employing such one-to-one diffusion dynamics, fully connected networks were only estimated to be 3% slower to recombination compared to networks of the same population size (GLM, $\exp(\beta)=1.033$, $t=6.808$, $p<.001$; **Table. S1**). Again, larger populations had a significantly shorter average time to recombination compared to smaller networks of the same architecture and degree (GLM, $\exp(\beta)=0.595$, $t=-109.094$, $p<.001$; **Fig. 2B, Table. S2**). However, under one-to-one diffusion, the relative times to recombination of different architectures was generally more consistent than under one-to-many diffusion, both in their median times to recombination (**Fig. 2B**) and in their relative performance under a given population size and level of connectivity (**Fig. 3B**). Within a given population size, multilevel architecture typically had the shortest times to recombination when networks had greater connectivity, but there was almost no difference in performance among architectures when connectivity was low (**Fig. 3B**). Thus, in contrast to one-to-many, one-to-one diffusion increased the tempo for architectures with greater modularity and clustering (modular, modular lattice, multilevel) relative to the other architectures.

Model 2 also tracked the time for the recombination product to diffuse to the majority of the population, something which model 1 was not designed to track. The time from recombination to diffusion was shortest in fully connected networks, and increased with population size (**Fig. 2C**). When evaluating performance from the start of the simulations until the time to diffusion, population size was the main contributor to differences in outcomes (**Fig. S5**). In small populations, the contribution of the final diffusion was relatively small compared to the time to recombination, meaning that the best performing networks in achieving recombination also performed best overall (**Fig. 3C**). By contrast, in larger populations, the performance of modular and clustered network architectures (modular, modular lattice, and multilevel) all performed worse: they were the slowest at reaching final diffusion (**Fig. 3C**) despite typically reaching

recombination the fastest (**Fig. 3B**). These differences, however, remain minor relative to the variance in outcomes within each set of conditions (architecture, population size and connectivity).

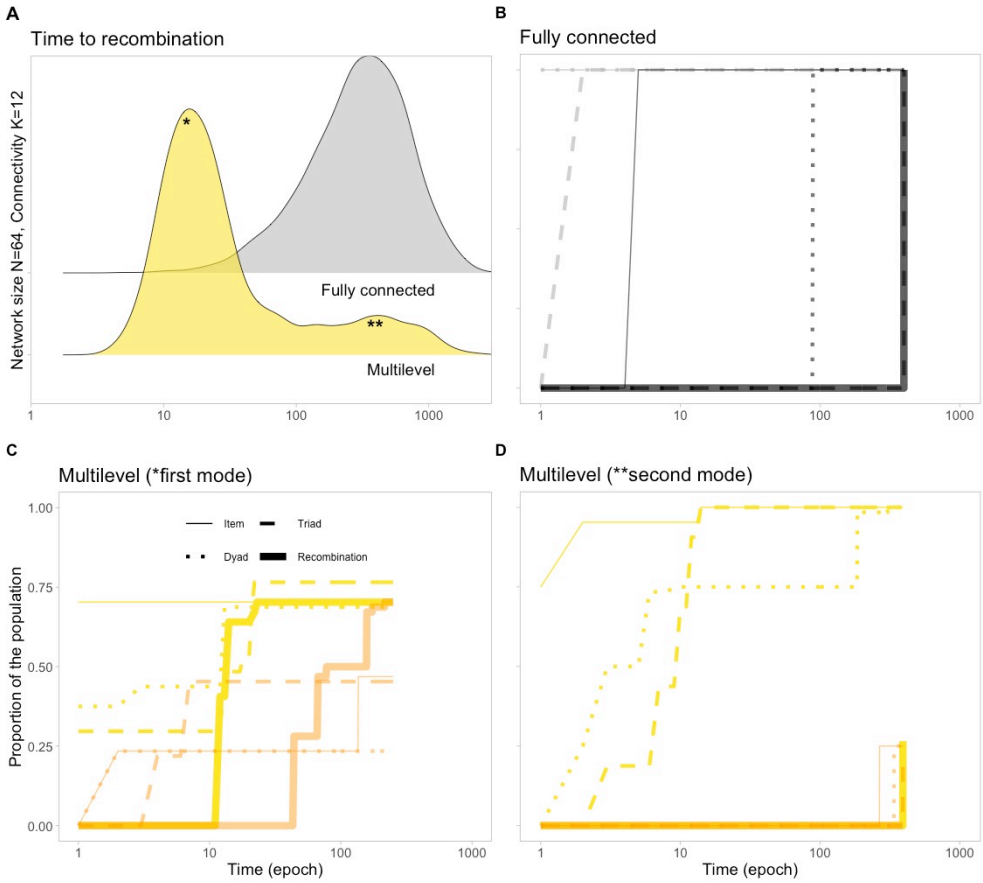

Figure 4. Cultural product diversity across time in a fully connected network and a highly structured social network architecture illustrates how early stochasticity shapes cultural outcomes. (A) Time to recombination (epochs) from 5,000 simulations with one-to-many diffusion dynamics (model 1) in multilevel and fully-connected networks (with N=64 and K=12). Following panels show cultural diversity over time from one simulation taken from the **(B)** from the mode of the fully-connected network, and the **(C)** first (*) and **(D)** second (**) modes of the distribution of results from the multilevel architecture. Cultural diversity represents the proportion of the population with one of the four possible products over time, from two independent lineages (light and dark shades): a single inventory item (1st stage; thin lines), a combination of two items (2nd stage; dotted lines), a valid combination triad of items (3rd stage; dashed lines), and the final higher payoff product, i.e. a triad recombining products from the two lineages (recombination; thick full lines).

Discussion

We revisit recent empirical and *in silico* experiments in humans to tease apart the contributions of different candidate social structures to the tempo of cumulative cultural evolution. Our results suggest that it is unlikely that one specific social network architecture consistently promotes CCE

251 across all population sizes, densities of social connections, or diffusion mechanisms. Rather, the
252 relationship is nuanced; the broad distribution of outcomes from our two models indicate that the
253 best performing architecture under some conditions can be the worst performing architecture
254 under others. Further, the outcome of any diffusion mechanism is as likely to be affected by
255 stochastic processes as by the architecture of the networks itself. While not at odds with previous
256 work showing that multilevel societies can accelerate CCE [19], our results suggest that a range of
257 other partially connected architectures could equally increase the tempo of CCE.
258
259 The fact that alternative architectures can have similar outcomes in terms of CCE has important
260 consequences for how the social structure of societies and CCE are framed in future discussions,
261 and where future research is directed. Current thinking is that complex, highly structured
262 societies, such as multilevel societies, might precede recombinatory CCE in the timeline of human
263 evolution, or that the benefits accrued from cultural evolution [22] or CCE [19] might co-evolve
264 with clustered and modular network structures. However, our results suggest that simple patterns
265 of spatial distribution (e.g. a lattice social network caused by distributed resources) could lead to
266 largely equivalent effects on CCE. It follows that we might expect to find recombinatory CCE even
267 before the evolution of complex societies. Indeed, evidence that simple, lattice-like social
268 structures [24] can provide a substrate for recombinatorial culture might be provided by the
269 combinatorial, spatially variable song structure of territorial passerine birds [25-29], which several
270 authors have proposed to be a simple form of CCE [30,31].
271
272 Population size has been suggested as another major demographic factor affecting rates of CCE
273 [3,7-9]. Our findings confirm this previous research, with our simulations showing that larger
274 populations always have a higher rate of cultural accumulation. Population size also interacted
275 with connectivity (which we modelled as a fixed network degree, i.e. the number of individuals'
276 social connections [22]), with changes in connectivity having a more pronounced effect in smaller
277 populations. This outcome is likely to arise because an increase in one unit of mean degree
278 corresponds to a greater increase in network connectivity in smaller populations (more rapidly
279 pushing the network towards becoming fully connected). However, in our simulations we did not
280 vary the distribution in connectivity among individuals, which has previously been shown to

impact the properties of information cascades [32] and differences among groups in behaviours such as cooperation [33]. Skewed degree distributions, where some nodes are much more connected than others, could allow independent lineages to arise in peripheral nodes and for highly connected 'hubs' to combine the products from these lineages, thereby facilitating CCE. Thus, variation in how much or how little individuals are connected, independently of other factors (mean connectivity, population size, and network properties), is an important dimension for future studies on CCE to consider.

Fully connected networks have been commonly used to evaluate the performance of a transmission network with a given set of characteristics [3,19]. Our simulations demonstrate that the contribution of large differences in connectivity outweighs any effects pertaining to architecture, at least when information is broadcast (i.e. a one-to-many diffusion mechanism). Further, for most human societies, a fully-connected social network for a population of any reasonable size would correspond with an unrealistically high level of connectivity [34], even in the higher levels of the fractal-like human social networks [35]. Thus, we suggest that fully connected networks are uninformative null models for testing the influence of social structure on rates of CCE. Instead, random networks of similar sizes and densities of connections as a given network of interest would provide a more robust benchmark for comparing the performance of its architecture. Our results suggest, however, that any effect of network architecture on increased rate of CCE inferred from noisy field data would likely be indistinguishable from the null expectancy, as variation within architecture greatly exceeded that between architectures.

The evolutionary benefits of CCE not only rely on cultural accumulation, but also on the ability for new cultural traits to spread through populations. When we extended simulations to examine the time from recombination to the diffusion of the final higher payoff product, our results suggested that the network architecture hypothesized to improve time to recombination performance paradoxically inhibited diffusion most. These findings complement and extend the previous study by Derex et al. [12] demonstrating that populations with partially-connected network structures can suffer from cultural loss when connectivity becomes too low for new innovations to spread. Further, the relative performance of architectures can change dramatically when considering

311 performance in terms of acquisition of behaviour by the majority of nodes in a network, as
312 opposed to the time when a single node has reached recombination, especially in larger
313 populations. For example, while multilevel architecture consistently reached recombination faster
314 than random networks under one-to-one diffusion, this architecture then restricted the final
315 spread of higher-value cultural traits. Our results therefore suggest that multiple dimensions of
316 performance—including every step from innovations to the final acquisition of higher-valued
317 traits—may need to be considered when studying the role of social structure in shaping CCE and
318 vice-versa.
319
320 Our work reinforces the need for studies of CCE to explicitly consider how network structure
321 interacts with transmission mechanisms to form a realised transmission network. We show that a
322 very restrictive transmission dynamics (one-to-one) mitigates the effect of network connectivity on
323 CCE by generating a partially connected transmission network within an otherwise fully-
324 connected social network. The consequences of transmission dynamics on CCE were
325 demonstrated, for instance, by Migliano et al. [19] who found that CCE was faster in simulations
326 where transmission was limited to kin-based connections (i.e. reduced connectivity). Under one-
327 to-one diffusion, independent lineages can develop in fully-connected networks because new
328 information is not immediately accessible to all, leading to more comparable performance between
329 fully and partially connected networks. Thus, when simulating CCE, it is important to match the
330 transmission dynamics with the time scale of the model. One-to-many diffusion can be realistic
331 when each epoch represents one generation (e.g. the innovation of a new medicine [19] could take
332 tens or hundreds of epochs to reach high recombinatory levels), while the one-to-one diffusion
333 might be more realistic when cultural traits are simpler to recombine. The production and
334 innovation frequency, as well as transmission biases, may further vary between species,
335 populations, tasks and contexts. Together with network structure, innovation frequency and
336 transmission biases may fundamentally alter the transmission dynamics—for example, conformity
337 overrides pay-off biases [21,36] and homophily reduces social connectivity [18,37]—fuelling
338 evolutionary feedbacks between network structure and cultural evolution [22]. Both factors will
339 therefore alter the resulting transmission networks, potentially restricting spread of new cultural
340 traits and slowing recombinatory CCE. More than highlighting the intricate, yet nuanced,

341 interplay between demography and cultural transmission, our work strengthens our emerging
342 understanding that realised connectivity, rather than network architecture, is important for CCE
343 [2,3].
344
345 **Materials and Methods**
346
347 *Networks*
348
349 We generated six architectures of binary social networks in which nodes represent individuals
350 linked by social relationships: (i) small-world networks, using the Watts-Strogatz model [23] with
351 node degree *K* links; (ii) random networks, by randomly connecting nodes ensuring all nodes had
352 the same degree *K*; (iii) lattices, by placing nodes on a grid and connecting each to its *K* nearest
353 neighbours; (iv) modular networks, by assigning nodes into nine modules, randomly connecting
354 each to *K-1* nodes from the same module and one node from another module; (v) modular lattices,
355 as per modular networks, but where the connections within modules were lattices; and (vi)
356 multilevel networks, as per modular lattices, but assigning nodes into three sets of three modules,
357 and connecting each to *K-2* nodes within their module, one node from each module from within its
358 set and one node from a module outside of it. We generated networks with different sizes
359 ($N \in \{64,144,324\}$ nodes), and densities of connections (in which $K \in \{8,12,18,24,30\}$ average links).
360 We used these population sizes because they allowed us to partition the network into equally-
361 sized clusters composed of equally-sized groups in which all individuals had the same degree, and
362 in which connectivity was greater within groups and within clusters than between groups and
363 between clusters.
364
365 *Network metrics*
366
367 Although all networks had comparable sizes and densities (i.e. the proportion links), the six
368 architectures varied in levels and combinations of clustering coefficient and modularity.
369 Clustering, *C*, informs the tendency of connected nodes to share the same connections with other

nodes, while modularity, Q, informs the tendency of the nodes to be organized into cohesive subsets that are more connected to each other than to the rest of the network [38].

Simulations

Our first agent-based model (model 1) followed Migliano et al. [19]. All agents were initialized with an inventory of three items from each of two lineages. In each simulation round (epoch), each focal agent was selected once, at random, and a partner randomly chosen from its social network connections. These agents combined one or two items from their inventory in proportion to their value into a triad of items. If this triad was a valid product, knowledge of that product was learned, spread immediately to all their network connections (one-to-many diffusion), and subsequently became available as an ingredient for making new products. Simulations finished once a recombination product (a triad that recombines specific products from both lineages) was first innovated. We ran 5,000 simulations for each of the network architecture types, sizes and densities of connections, recording time to achieve the recombination product (in epochs) and diversity of innovations in each epoch. An epoch was one simulation round in which each agent was selected once as a focal agent in random order.

Our second agent-based model (model 2) extended the first by changing the transmission mechanic and altering the set of valid combinations such that the model can run past the first innovation of either recombination product. Transmission of valid products now occurred between dyads of agents (one-to-one diffusion) prior to choosing items from their inventory, in contrast to the broadcast style of diffusion in model 1. Secondly, if a triad contained either recombination products, the final product was that recombination product. In the case where both recombination products were present in the triad, one was chosen as the final product at random. This allowed us to track the diffusion of recombination products beyond their innovation. We also ran 5,000 simulations for the same parameter space of model 1, recording time to recombination and time to diffusion to the majority of the network (in epochs). We implemented the agent-based models in R and Python. The code to generate the social networks, perform the simulations, the statistical analyses and the figures are available at [39]

400

401 *Data analyses*

402

403 To compare the performance of agents organized in different network architectures, we used time-
404 to-event (survival) analyses [40] where time to recombination was a function of architecture and
405 connectivity. For each population size, we used the Cumulative Incidence Function to estimate the
406 proportion of simulations in which agents reached the recombination of each cultural lineage's
407 products into a final high-payoff product. We used the non-parametric Kaplan-Meier product
408 limit estimator to represent the time intervals based on observed recombination events from 5,000
409 simulations from model 1, calculating 95% confidence intervals with the Greenwood estimator. To
410 measure variance in time to recombination across population sizes, we measured the quartile
411 coefficient of dispersion (QCD=(Q3-Q1)/(Q3+Q1)), as this variable is not normally distributed and
412 QCD offers a more robust measure.

413

414 While statistics are not typically performed on data from agent-based models since the posterior is
415 directly sampled, we wanted to quantify the relative contributions of architecture, size and
416 connectivity without the cumbersome descriptions of the entire distribution (which can be readily
417 seen in **Fig. 2)**. For both models 1 and 2, we created three sets of generalized linear models (GLMs)
418 that predicted logged time to recombination (in epochs). Time to recombination was logged to
419 account for non-normality of residuals, and to make comparisons more fair by bringing the mean
420 closer to the median of the distribution. All models used log link function, as the data was non-
421 linear conditional on predictors, even after the log transformation. Also, the log link function
422 allowed the presentation of exponentiated coefficients, which simplify the comparison to the
423 reference (here, the random networks at the GLM intercept). The first set of GLMs used a full
424 interaction structure to partition the relative contributions of architecture, size and connectivity to
425 average time to recombination **(Table S1)**, excluding fully connected networks. To then compare
426 fully connected networks to all other networks, we built a GLM using architecture and population
427 size as predictors in a full interaction structure **(Table S2)**. Connectivity was excluded as a
428 predictor, as all fully connected networks only have 1 possible degree ($K=N-1$). Finally, to compare
429 differences between architectures in **Fig. 3** more precisely, we subset data by connectivity and

population size and performed a GLM with only architecture as a predictor for each subset, again excluding fully connected networks. We performed all data analyses in R [41], using 'survival' [42] and 'survminer' [43] packages.

Competing interests

The authors have no competing interests with this study

Acknowledgments

We thank the Social Evolutionary Ecology Lab and the Cognitive and Cultural Ecology Lab for the discussion that inspired this manuscript. This work was funded by the Max Planck Society. DRF and DP were funded by a grant from the European Research Council (ERC) under the European Union's Horizon 2020 research and innovation programme (grant agreement No. 850859), awarded to DRF. LMA was funded by a Max Planck Independent Group Leader Fellowship. PH was funded by a scholarship from the China Scholarship Council (No. 201706100183). M.C. was funded by CAPES (88881.170254/2018-01). This work was supported by the Max Planck Society, and the Advanced Centre for Collective Behaviour, funded by the Deutsche Forschungsgemeinschaft (DFG, German Research Foundation) under Germany's Excellence Strategy (EXC 2117–422037984).

References

1. M. Tomasello, The human adaptation for culture. *Annual Rev. Anthrop.* **28(1),** 509-529 (1999).

2. A. Mesoudi, A. Thornton, What is cumulative cultural evolution? *Proc. R. Soc. B.* **285(1880)**, 20180712 (2018).

3. M. Derex, A. Mesoudi, Cumulative cultural evolution within evolving population structures. *Trends Cogn. Sci.* (In press).

4. R. Boyd, P.J. Richerson, *The origin and evolution of cultures*. Oxford University Press, Oxford (2005).

460 5. R. Boyd, P.J. Richerson, J. Henrich, The cultural niche: Why social learning is essential for
461 human adaptation. *Proc. Natl. Acad. Sci.* **108**, 10918–10925 (2011).
462 6. S. Shennan, Demography and cultural innovation: a model and its implications for the
463 emergence of modern human culture. *Cambridge Arch. J.* **11(1)**:5-16 (2001).
464 7. J. Henrich, Demography and cultural evolution: How adaptive cultural processes can produce
465 maladaptive losses—the Tasmanian case. *Am. Antiq.* **69(2)**, 197–214 (2004).
466 8. A. Powell, S. Shennan, M.G. Thomas, Late Pleistocene demography and the appearance of
467 modern human behavior. *Science* **324(5932)**, 1298–1301 (2009).
468 9. M. Derex, M.-P. Beugin, B. Godelle, M. Raymond, Experimental evidence for the influence of
469 group size on cultural complexity. *Nature* **503(7476),** 389–391 (2013).
470 10. N. Fay, N. de Kleine, B. Walker, C.A. Caldwell, Increasing population size can inhibit
471 cumulative cultural evolution. *Proc. Natl. Acad. Sci.* **116(14)**, 6726-6731 (2019).
472 11. J. P. Martens, Scenarios where increased population size can enhance cumulative cultural
473 evolution are likely common. *Proc. Natl. Acad. Sci.* **116(35),** 17160-17160 (2019).
474 12. M. Derex, R. Boyd, Partial connectivity increases cultural accumulation within groups. *Proc.*
475 *Natl. Acad. Sci.* **113(11)**, 2982-2987 (2016).
476 13. R. Baldini, Revisiting the effect of population size on cumulative cultural evolution. *J. Cogn.*
477 *Cult.* **15(3-4)**, 320-336 (2015).
478 14. M. Derex, C. Perreault, R. Boyd, Divide and conquer: intermediate levels of population
479 fragmentation maximize cultural accumulation. *Phil. Trans. R. Soc. B* **373(1743)**, 20170062 (2018).
480 15. J. Henrich, R. Boyd, M. Derex, M.A Kline, A. Mesoudi, M. Muthukrishna, A.T. Powell, S.J.
481 Shennan, M.G. Thomas, Understanding cumulative cultural evolution. *Proc. Natl. Acad. Sci.*
482 **113(44)**, E6724-E6725 (2016).
483 16. B. Voelkl, R. Nöe, The influence of social structure on the propagation of social information in
484 artificial primate groups: a graph-based simulation approach. *J. Theor. Biol.* **252(1)**, 77-86 (2008)
485 17. C.L. Nunn, P.H. Thrall, K. Bartz, T. Dasgupta, C. Boesch, Do transmission mechanisms or social
486 systems drive cultural dynamics in socially structured populations? *An. Behav.* **77(6)**,*15*15-1524
487 (2009).
488 18. M. Cantor, H. Whitehead, The interplay between social networks and culture: theoretically and
489 among whales and dolphins. *Phil. Trans. R. Soc. B* **368(1618)**, 20120340 (2013).

19. A.B. Migliano, F. Battiston, S. Viguier, A.E. Page, M. Dyble, R. Schlaepfer, D. Smith, L. Astete, M. Ngales, J. Gomez-Gardenes, V. Latora, Hunter-gatherer multilevel sociality accelerates cumulative cultural evolution. *Science Adv.* **6(9)**, p.eaax5913 (2020).

20. H. Whitehead, D. Lusseau, Animal social networks as substrate for cultural behavioural diversity. *J. Theor. Biol.* **294**,19-28 (2012).

21. L.M. Aplin, D.R. Farine, J. Morand-Ferron, A. Cockburn, A. Thornton, B.C. Sheldon, Experimentally induced innovations lead to persistent culture via conformity in wild birds. *Nature* **518(7540),** 538-541 (2015).

22. M., Smolla, E. Akçay, Cultural selection shapes network structure. *Sci. Adv*. **5(8)**, eaaw0609 (2019).

23. D.J. Watts, S.H. Strogatz, Collective dynamics of 'small-world' networks. *Nature* **393(6684)**, 440-442 (1998)

24. J.A. Firth, B.C. Sheldon, Social carry-over effects underpin trans-seasonally linked structure in a wild bird population. *Ecol. Lett.* **19(11),** 1324-1332 (2016).

25. J.P. Hailman, M.S. Ficken. Combinatorial animal communication with computable syntax: chick-a-dee calling qualifies as 'language' by structural linguistics. *An. Behav* **34**, 1899–1901 (1986).

26. L.L. Bloomfield, I. Charrier, C.B. Sturdy, Note types and coding in parid vocalizations. II: The chick-a-dee call of the Mountain Chickadee (*Poecile gambeli*). *Can. J. Zool.* **82**, 780–793 (2004).

27. D.E. Kroodsma, Winter Wren singing behavior: a pinnacle of song complexity. *Condor* **82**, 357–365 (1980).

28. D.W. Leger, First Documentation of combinatorial song syntax in a suboscine passerine species. *Condor* **107(4)**, 765–774 (2005).

29. C.L. Branch, V.V. Pravosudov, Mountain chickadees from different elevations sing different songs: acoustic adaptation, temporal drift or signal of local adaptation?. *R. Soc. Open Sci* **2.4,** 150019 (2015).

30. L. M. Aplin, Culture and cultural evolution in birds: a review of the evidence. *Anim. Behav.* **147**, 179-187 (2019).

31. A. Whiten, Cultural evolution in animals. *Ann. Rev. Ecol. Evol. System.* **50,** 27-48 (2019).

519 32. D.J. Watts, A simple model of global cascades on random networks. *Proc. Natl. Acad. Sci.* **99(9)**,
520 5766-5771 (2002).
521 33. C.L. Apicella, F.W. Marlowe, J.H. Fowler, N.A. Christakis, Social networks and cooperation in
522 hunter-gatherers. *Nature* **481(7382)**, 497-501 (2012).
523 34. B.J. West, G.F. Massari, G. Culbreth, R. Failla, M. Bologna, R.I.M. Dunbar, P. Grigolini, Relating
524 size and functionality in human social networks through complexity. *Proc. Natl. Acad. Sci.*
525 **117(31)**, 18355-18358 (2020).
526 35. R.I.M. Dunbar, Structure and function in human and primate social networks: implications for
527 diffusion, network stability and health. *Proc. R. Soc. A* **476**:20200446 (2020).
528 36. K.K. Denton, Y. Ram, U. Liberman, M.W. Feldman, Cultural evolution of conformity and
529 anticonformity. *Proc. Natl. Acad. Sci.* (In press).
530 37. M. McPherson, L. Smith-Lovin, J.M. Cook, Birds of a feather: Homophily in social networks.
531 *Annual Review of Sociology*, **27(1)**, 415-444 (2001).
532 38. M. Newman, *Networks*. Oxford University Press (2018).
533 39. M. Cantor, M. Chimento, S.Q. Smeele, P. He, D. Papageorgiou, L.M. Aplin, D.R. Farine. 2020.
534 Social network architecture and the tempo of cumulative cultural evolution. Github repository.
535 https://github.com/simeonqs/Social_network_architecture_and_the_tempo_of_cumulative_c
536 ultural_evolution
537 40. R.G. Miller Jr, *Survival analysis* (Vol. 66). John Wiley & Sons (2011).
538 41. R Core Team. R: A language and environment for statistical computing. R Foundation for
539 Statistical Computing, Vienna, Austria. URL https://www.R-project.org/ (2019).
540 42. T. Therneau, A Package for Survival Analysis in R. R package version 3.2-3, https://CRAN.R-
541 project.org/package=survival (2020)
542 43. A. Kassambara, M. Kosinski, P. Biecek, Survminer: Drawing Survival Curves using 'ggplot2'. R
543 package version 0.4.7. https://CRAN.R-project.org/package=survminer (2020)

Supporting Material for:

Social network architecture and the tempo of cumulative cultural evolution

Mauricio Cantor*, Michael C. Chimento, Simeon Q. Smeele, Peng He, Danai Papageorgiou, Lucy M. Aplin*, Damien R. Farine

Corresponding Authors: * Mauricio Cantor. Department for the Ecology of Animal Societies, Max Planck Institute of Animal Behavior, Am Obstberg 1, Radolfzell 78315, Germany; * Lucy M. Aplin. Cognitive & Cultural Ecology Research Group, Max Planck Institute of Animal Behavior, Am Obstberg 1, Radolfzell 78315, Germany, Phone: +49 7732 1501-13. **Emails:** mcantor@ab.mpg.de, laplin@ab.mpg.de

Table S1. Generalized linear models (GLMs) for agent-based model 1 (with one-to-many diffusion mechanism) and model 2 (one-to-one diffusion), in which time to recombination (time to recombination, measured as log(epoch+1)) is predicted by an interaction between population size and architecture. Coefficients and standard errors are exponentiated, as these GLMs used a log link function. Connectivity was not included, as this contains the same information as population size for fully connected networks. Intercepts represents random networks of population size N=64. (*p<0.1; **p<0.05; ***p<0.01)

	model1		model2	
	Estimate	p-value	Estimate	p-value
Constant	3.425***	-0.003	4.205***	-0.002
graphsmall_world	0.999***	-0.004	1.003***	-0.002
graphlattice	1.010***	-0.004	1.013***	-0.002
graphmodular	0.970***	-0.004	0.994***	-0.002
graphmodular_lattice	0.972***	-0.004	0.991***	-0.002
graphmultilevel	0.977***	-0.004	0.982***	-0.002
graphfull	1.652***	-0.003	1.033***	-0.003
pop_size144	0.715***	-0.004	0.759***	-0.002
pop_size324	0.512***	-0.004	0.587***	-0.003
graphsmall_world:pop_size144	0.999***	-0.005	0.999***	-0.003
graphlattice:pop_size144	0.996***	-0.005	0.989***	-0.003
graphmodular:pop_size144	1.013***	-0.005	0.996***	-0.003
graphmodular_lattice:pop_size144	0.999***	-0.005	1.003***	-0.003
graphmultilevel:pop_size144	1.024***	-0.005	1.011***	-0.003
graphfull:pop_size144	1.206***	-0.005	0.994***	-0.005
graphsmall_world:pop_size324	1.005***	-0.006	0.997***	-0.004
graphlattice:pop_size324	1.012***	-0.006	0.986***	-0.004
graphmodular:pop_size324	1.059***	-0.006	1.001***	-0.004
graphmodular_lattice:pop_size324	1.036***	-0.006	1.006***	-0.004
graphmultilevel:pop_size324	1.100***	-0.006	1.015***	-0.004
graphfull:pop_size324	1.406***	-0.006	0.980***	-0.005
Observations	345,000		345,000	
Log Likelihood	-446,718.40		-378,097.40	
Akaike Information Criterion	893,478.70		756,236.80	

564 **Table S2.** Generalized linear models (GLMs) for agent-based model 1 (with one-to-many
565 diffusion mechanism) and model 2 (one-to-one diffusion), in which time to recombination
566 (time to recombination, measured as log(epoch+1)) is predicted by an interaction between
567 population size, network architecture, and connectivity (i.e. average network degree).
568 Coefficients and standard errors are exponentiated, as these GLMs used a log link function.
569 Full networks were excluded. Intercepts represent random networks of population size N=64,
570 average degree of K=8. (*p<0.1; **p<0.05; ***p<0.01)
571

	model1		model2	
	Estimate	p-value	Estimate	p-value
Constant	3.196***	-0.004	4.168***	-0.002
graphsmall_world	0.999***	-0.005	1.009***	-0.003
graphlattice	1.010***	-0.005	1.011***	-0.003
graphmodular	1.005***	-0.005	1.006***	-0.003
graphmodular_lattice	1.011***	-0.005	1.004***	-0.003
graphmultilevel	1.020***	-0.005	0.993***	-0.003
pop_size144	0.724***	-0.007	0.756***	-0.004
pop_size324	0.618***	-0.007	0.595***	-0.005
degree12	1.143***	-0.005	1.018***	-0.003
degree18	0.847***	-0.01	0.996***	-0.006
degree24	0.831***	-0.01	0.995***	-0.006
degree30	0.856***	-0.01	0.992***	-0.006
graphsmall_world:pop_size144	0.997***	-0.009	0.992***	-0.006
graphlattice:pop_size144	1.007***	-0.009	0.989***	-0.006
graphmodular:pop_size144	0.973***	-0.009	0.998***	-0.006
graphmodular_lattice:pop_size144	0.942***	-0.009	1.008***	-0.006
graphmultilevel:pop_size144	0.967***	-0.009	1.014***	-0.006
graphsmall_world:pop_size324	1.004***	-0.01	0.987***	-0.007
graphlattice:pop_size324	1.021***	-0.01	0.988***	-0.007
graphmodular:pop_size324	0.930***	-0.011	0.993***	-0.007
graphmodular_lattice:pop_size324	0.876***	-0.011	0.996***	-0.007
graphmultilevel:pop_size324	0.955***	-0.01	1.005***	-0.007
graphsmall_world:degree12	0.999***	-0.007	0.987***	-0.005
graphlattice:degree12	1.000***	-0.007	1.004***	-0.005
graphmodular:degree12	0.934***	-0.007	0.976***	-0.005
graphmodular_lattice:degree12	0.928***	-0.007	0.974***	-0.005
graphmultilevel:degree12	0.922***	-0.007	0.978***	-0.005
graphsmall_world:degree18	1.002***	-0.014	1.003***	-0.008
graphlattice:degree18	0.996***	-0.013	0.997***	-0.008
graphmodular:degree18	1.131***	-0.014	0.988***	-0.008
graphmodular_lattice:degree18	1.170***	-0.014	0.996***	-0.008
graphmultilevel:degree18	1.130***	-0.013	0.998***	-0.008
graphsmall_world:degree24	1.005***	-0.014	1.002***	-0.008
graphlattice:degree24	0.992***	-0.014	1.003***	-0.008
graphmodular:degree24	1.163***	-0.014	0.991***	-0.008
graphmodular_lattice:degree24	1.231***	-0.014	0.996***	-0.008
graphmultilevel:degree24	1.172***	-0.013	0.995***	-0.008
graphsmall_world:degree30	0.999***	-0.014	1.006***	-0.008
graphlattice:degree30	0.977***	-0.013	1.000***	-0.008
graphmodular:degree30	1.168***	-0.013	0.996***	-0.008
graphmodular_lattice:degree30	1.237***	-0.014	0.992***	-0.008
graphmultilevel:degree30	1.175***	-0.013	0.999***	-0.008
pop_size144:degree12	0.864***	-0.009	0.992***	-0.006
pop_size324:degree12	0.796***	-0.011	0.975***	-0.007
pop_size144:degree18	1.251***	-0.012	1.023***	-0.007
pop_size144:degree24	1.426***	-0.012	1.030***	-0.007
graphsmall_world:pop_size144:degree12	1.000***	-0.013	1.014***	-0.008
graphlattice:pop_size144:degree12	0.989***	-0.013	0.998***	-0.008
graphmodular:pop_size144:degree12	1.101***	-0.013	1.017***	-0.008
graphmodular_lattice:pop_size144:degree12	1.134***	-0.013	1.016***	-0.008
graphmultilevel:pop_size144:degree12	1.133***	-0.013	1.016***	-0.008
graphsmall_world:pop_size324:degree12	0.999***	-0.015	1.017***	-0.01
graphlattice:pop_size324:degree12	0.989***	-0.015	0.995***	-0.01
graphmodular:pop_size324:degree12	1.125***	-0.015	1.027***	-0.01
graphmodular_lattice:pop_size324:degree12	1.160***	-0.016	1.030***	-0.01
graphmultilevel:pop_size324:degree12	1.154***	-0.015	1.024***	-0.01
graphsmall_world:pop_size144:degree18	1.005***	-0.017	1.000***	-0.01

graphlattice:pop_size144:degree18	0.999***	-0.017	1.006***	-0.01
graphmodular:pop_size144:degree18	0.907***	-0.017	0.991***	-0.01
graphmodular_lattice:pop_size144:degree18	0.902***	-0.017	0.977***	-0.01
graphmultilevel:pop_size144:degree18	0.921***	-0.017	0.982***	-0.01
graphsmall_world:pop_size144:degree24	0.994***	-0.017	0.997***	-0.01
graphlattice:pop_size144:degree24	0.981***	-0.017	0.998***	-0.01
graphmodular:pop_size144:degree24	0.835***	-0.017	0.981***	-0.01
graphmodular_lattice:pop_size144:degree24	0.794***	-0.017	0.973***	-0.01
graphmultilevel:pop_size144:degree24	0.836***	-0.017	0.977***	-0.01
Observations	330,000		330,000	
Log Likelihood	-423,477.80		-359,565.20	
Akaike Information Criterion	847,087.60		719,262.30	

572

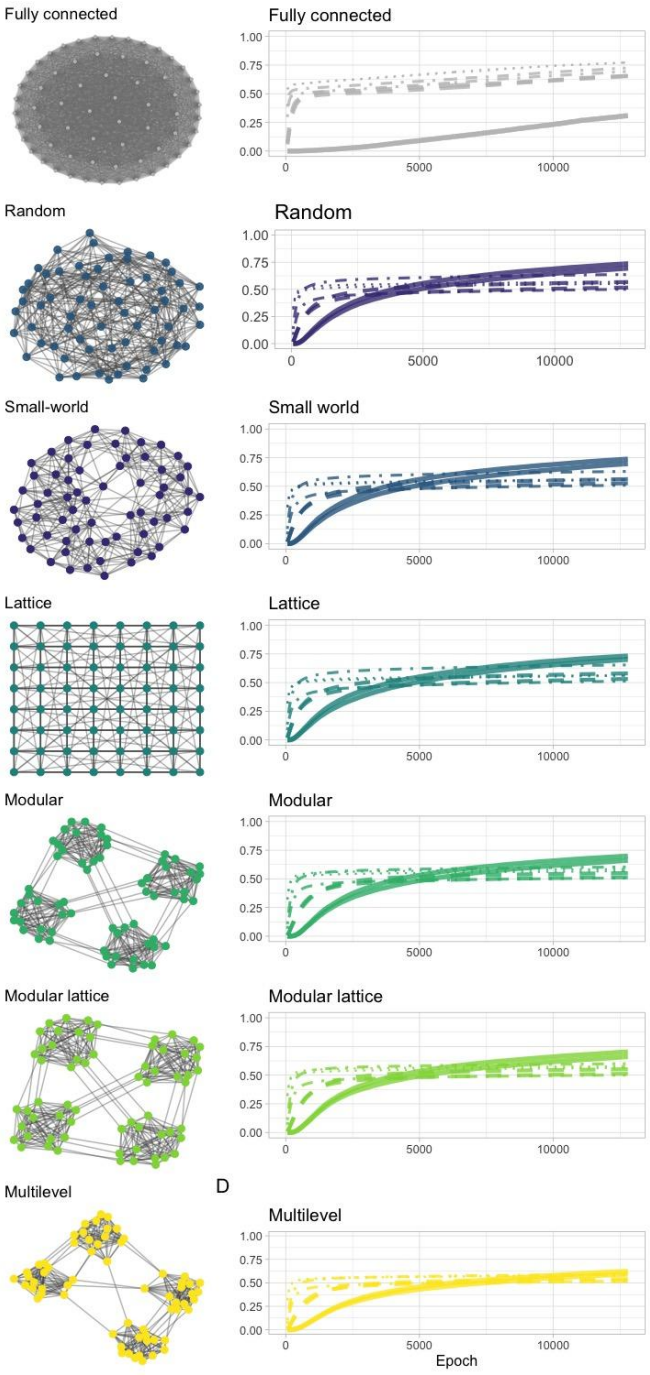

D

573

574 **Figure S1. Cultural trait diversity across social network architectures and proposed null**
575 **models.** Comparison of the diversity of cultural traits along the network architecture
576 spectrum, across populations of same size (N=64 nodes) and connectivity (average degree
577 K=12 links) in relative to a fully connected network of the same size (N=64, K=63). Cultural
578 innovation diversity across network architectures measured as the proportion of the
579 population with one of the four possible traits over time: a single inventory item (dotted
580 lines), a single combination of two items (dashed and dotted lines), a valid combination of
581 three items (triad; dashed lines), and a recombination product (a triad that recombines
582 specific products from both lineages; thick lines). The inventory items came from two
583 independent lineages, represented by lines of the same type.
584